ASV '94 A36
Third Asian Symposium
on Visualization

Flow Visualization of Tube Flow in a Heat Exchanger –The Effect of Mutural Position Between Inlet and Outlet of the Tube Arrays on the Distribution of the Flow Rate –

Shiro IKUTA
(Calsonic Co., Sano City, 327, *Japan*)
Mitunobu AKIYAMA and Hitoshi SUGIYAMA
(Utsunomiya University, Utsunomiya city, 321, *Japan*)

INTRODUCTION

This study aims to obtain uniform distribution of the flow rate in the tube arrays inside of a heat exchanger, so as to improve the heat transfer efficiency of the system. As the first step, the configurations[1] of branches and expect confluents[2] of the passages of the individual tubes are examined. Flow visualization by nylon-particle tracer method is applied for the water flow in the tube array model. A numerical simulation is also carried out on the model for comparison. The results show that the flow rates and patterns in the tube arrays are greatly dependent on the mutual position among the tube arrays in conjunction with the flow inlet and outlet of the model.

EXPERIMENTAL APPARATUS AND NUMERICAL METHOD

The water channel and the two-dimensional heat exchanger model are illustrated in Fig. 1 and Fig. 2, respectively. The water channel consists of pump, flow meters, water setting chamber, test core and exhaust chamber. The flow rate is regulated within 1.67×10^{-4} - 2.83×10^{-3}m^3/sec, the maximum velocity at the inlet of observing core is about 0.3 m /sec. The side of the observing core is a 200 mm × 190 mm rectangular section of the exchanger model made by transparency acryl resin.The two-dimensional heat exchanger model is composed of ten tubes. The width of tubes is 10 mm, and the length of tube arrays is relatively shorter than the distance between the inlet and outlet walls. In Fig. 2, tube number is counted in sequence from the inlet of test section.

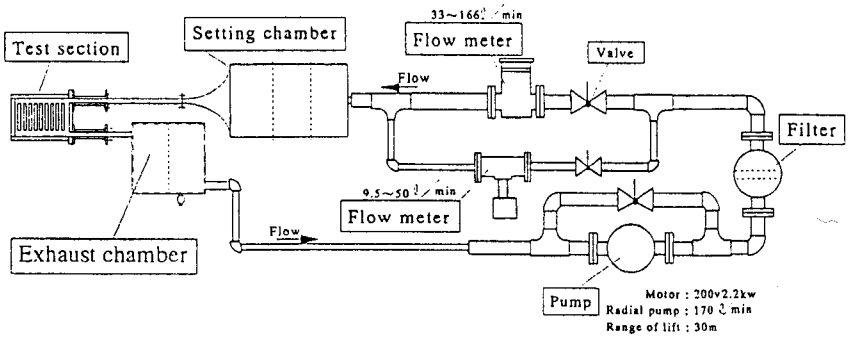

Fig.1 Experimental apparatus

The coordinate system for calculation is shown in Fig. 3. The governing equations are continuity equation (1) and Navier-Stokes equation (2). The governing equations are discretized by the CVM method, the convection and diffusion terms are expressed by the QUICK scheme, and the pressure correction term is solved by the SIMPLE method. The staggered grid is used in calculation with a 160 × 100 uniformmesh. Boundary conditions is also displayed in Fig. 3. The Reynolds number (hereafter designated Re) in this case is 495.

Continuty equation

$$\frac{\partial \rho \widetilde{Ui}}{\partial Xi} = 0 \quad (1)$$

Navier -Stokes equation

$$\frac{\partial \widetilde{Ui}}{\partial t} + \frac{\partial}{\partial Xk}(\widetilde{Ui}\,\widetilde{Uk}) = \frac{\partial}{\partial Xk}(\nu \frac{\partial \widetilde{Ui}}{\partial Xk}) - \frac{1}{\rho}\frac{\partial P}{\partial Xi} + g(\rho_1 - \rho_0) \quad (2)$$

$\widetilde{Ui}$: instantaneous velocity
T : temperature
P : pressure
t : time
X : length of X direction
Y : length of Y direction
ρ : density
ν : kinetic viscosity
λ : conductance
Cp : specific heat
β : thermal expansion coefficient
g : acceleration of gravity

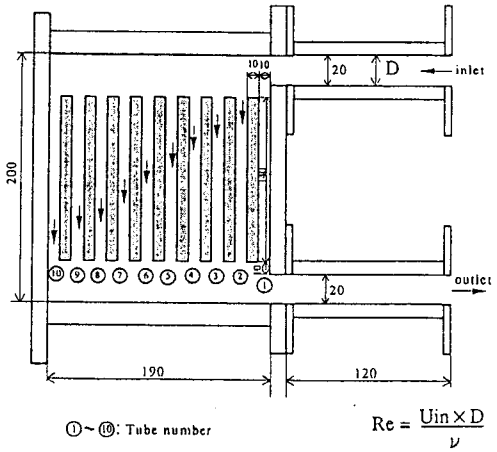

Fig.2 Type C Model core configuration

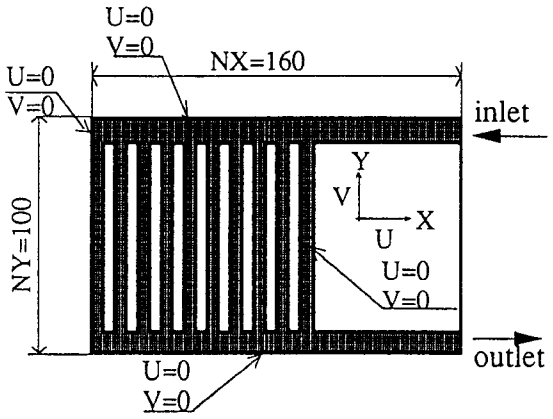

Fig.3 Grid and boundary condition

RESULTS AND DISCUTION

1) Flow visualization and numerical result

Flow pattern observed at the velocity of 0.025 m/s (Re = 495) is given in Fig.4. The flow at the inlet of observing core changes its direction to the entrance of tubes, impinging upon the second tube from the inlet and large amount of the fluid flows into that tube. The rest of the fluid enters the other tubes. The fluid flow along the upper walls of the inlet side stopes at the wall that located opposite to the inlet, where rotated flow occurs. The flow entered into the first tube comes from the backward flow which happened when the inlet flow impinges upon the solid walls among tubes. Compared with the flows of the other tubes, the flow towards the second tube goes directly, keeping the angle between flow and tube direction to be the smallest. As the result, the stream motion is very smooth and the maximum speed is obtained here. For the other tubes except for the second one, the angle mentioned above increases gradually. In fact, this angle becomes nearly 90 ° when tube number is bigger than 4. At the entrances of these tubes, reversed current areas, whose regions are about the same as the tube width, are observed.

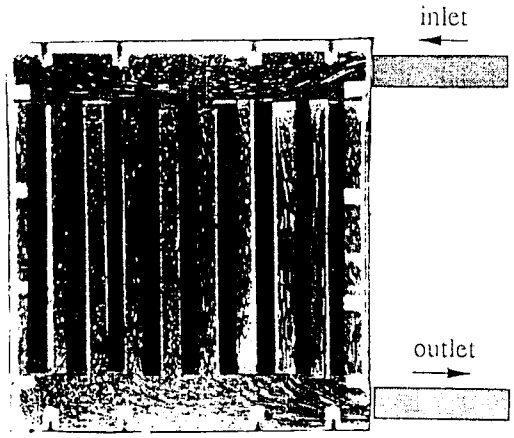

Fig.4 Flow pattern through tube arraies
Re=495(0.025m/s)

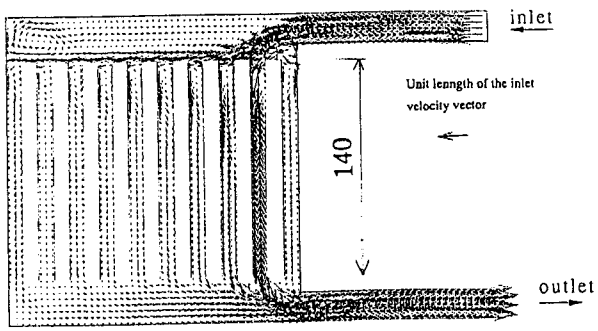

Fig.5 Velocity vector distribution
Re=495

Calculation result of the velocity vector is portrayed in Fig. 5 when the inlet flow velocity is 0.025 m/s. The velocity vector and the visualization result are found to be in good agreement. The comparison between the calculation and the experimental results of the flow rates in each tubes is shown in Fig. 6. Although these Re numbers of experiments and calculations are different, these results are in good agreement. The value of the flow rate in each of the branch passes divided by the total inflow is called the flow rate Φ.[3][4]

Fig.7 demonstrates the measuring results of the velocity distribution for each tubes when velocities of the inlet flow are 0.054 m/s and 0.100 m/s. The flow velocity of the second tube shows the maximum value, and its intensity decreases gradually with the increase of the tube number. If the tube arrays are arranged in this form, it is easy for the water flow to enter the second tube as the local entrance pressure is higher than those of the other tubes. It is also predicted that no large change is found in the flow rates distribution even if the inlet flow rate is increased.

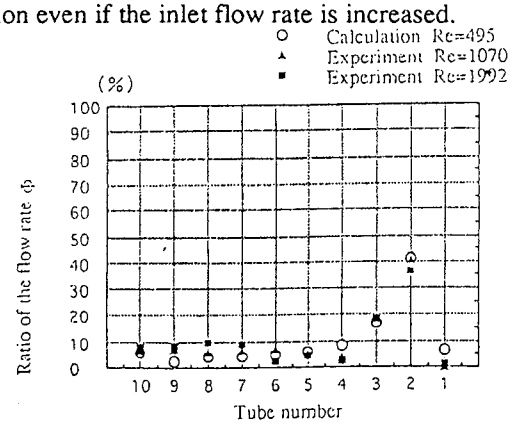

Fig.6 Flow rate distribution in tube arrays

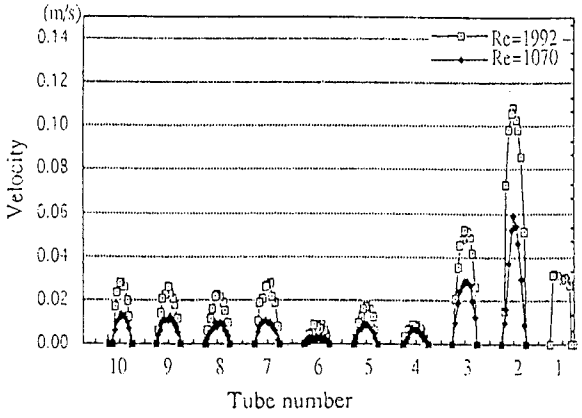

Fig. 7 Velocity distribution

2) Infulence of Inlet/Outlet ports

Fig.8 shows a two-dimensional model in which the inlet and outlet ports have been relocated. The inlet port was fixed, and outlet ports were laid on the right of the outlet chamber (Type C is shown as Fig. 2), the center (TypeT), and the left (Type I).

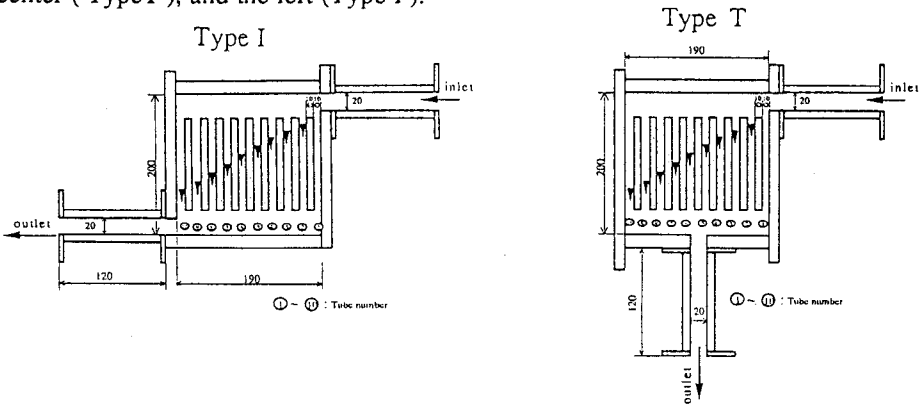

Fig.8 Location of Outlet Ports

Fig. 9 and Fig. 10 show the numerical velocity vector diagrams of these two types, respectively. The calculated Reynolds number has been defined to be 500 by using the inflow velocity and inlet port width for each type. The type C flow has been already described. The flow of the type I is as follows. After the flow entering the inlet chamber, the main flow goes down to the 10th branch pass, which accomodates most of the main flow, with small amounts of the liquid flowing into the third and later branch passes. The 1st and 2nd branch passes receive only a negligible amount of the flow. The typeT flow is as follows. Most of the upstream liquid flow enters the 4th and 5th branch passes. The flow decreases in the directions of the 1st and 10th branch passes. Almost none of the main flow enters the 1st or 2nd branch passes.

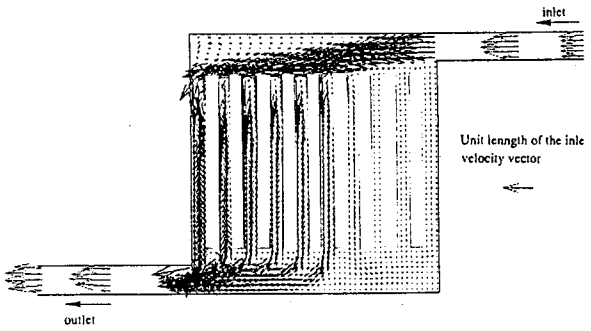

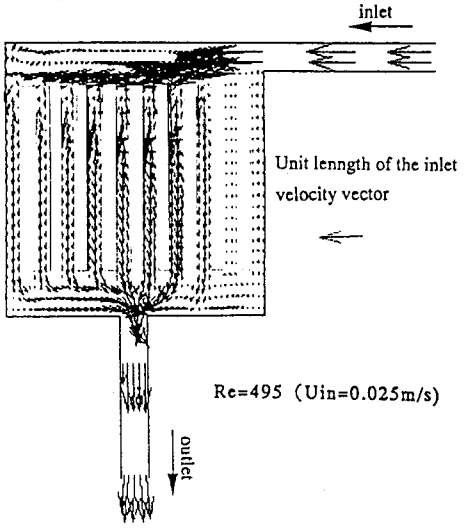

Fig.9 Velocity distribution in Type I

Fig.10 Velocity distribution in Type T

By calculating the flow ratio for each branch pass, the flow rate distribution for the branch passes can be determined. Fig.11 shows the comparison of the flow rate distribution for each type. By the above observation results in the type C structure, it is indicated that 40 % of the total flow rate is received by the 2nd branch pass. Only 6 % of the total flow rate occurs at the sixth and later branch passes, indicating that the type C dose not provide a uniform flow rate distribution. For the type I, we found the following flow rate results. The maximum inflow rate is at the 10th branch pass, which accounts for 25 % of the total flow rate. As the flow approaches the 1st branch pass, the flow rate decreases until it becomes zero or negative at these branch passes. This indicates that the forward flow ceases flowing or even reverses at the 1st and 2nd branch passes. The above findings indicate that changing the location of the outlet ports in the outlet chamber cannot realize the uniform flow of each passes.

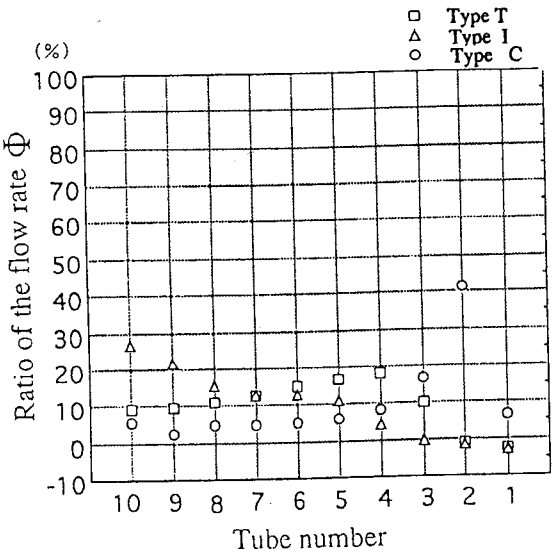

Fig. 11 Flow rate distribution

3) Influence of Pass Length

To determine the effects of the pass length on drift , we changed the length of the passes and conducted a new set of observations.To examine the flow and the flow velocity distribution in a branch pass, we obtained the velocity vector and the velocity of the flow from the results of numerical calculations and comparedthose results each other. The velocity vector for each model are shown in Fig. 12 (pass length 160 mm), Fig. 13 (140 mm), Fig. 14 (100 mm) and Fig. 15 (10 mm). As the length of the series of passes gradually decreases, separation vortex can be observed constantly in the inlet chamber, indicating that drift has not been improved.In the outlet chamber, flows from the 1st throught 10th branch passes run together into layers. Increasing in velocity, these layered flows then reach the outlet port and exit chamber. Moreover, in order to realized the uniform distribution of the flow rate,the volume of outlet chamber is set to larger than that of inlet chamber by moving the tube location. Picture of the test for pass length of 140 mm was obtained. Photo.1 is for pass length of 140 mm.The photograph mat-

ches the appropriate calculation result satisfactorily. Fig. 16 shows the calculated results for outlet chambers of different sizes. Fig. 16 is for a passlength of 140 mm. In this case, the flow rate distribution in the branch passes is relatively uniform, indicating the decrease in drift. At the same time this characteristic feature is confirmed by the experimental results presented in photo. 1.

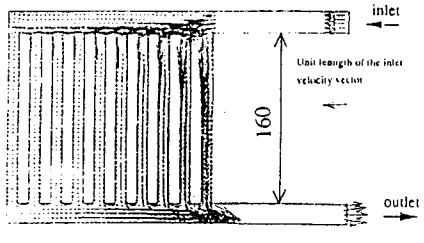

Fig. 12 Velocity vector distribution (pass length 160 mm) Re = 500

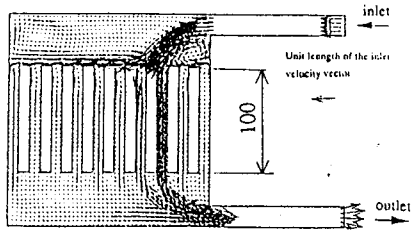

Fig. 14 Velocity vector distribution (pass length 100 mm) Re = 500

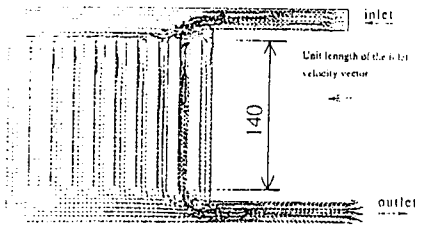

Fig. 13 Velocity vector distribution (pass length 140 mm) Re = 500

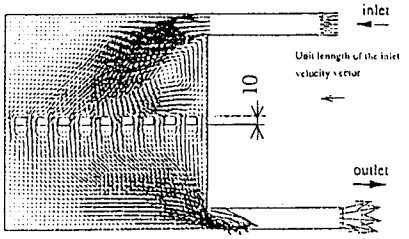

Fig. 15 Velocity vector distribution (pass length 10 mm) Re = 500

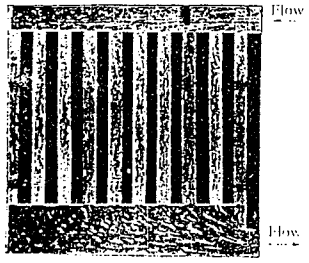

Phot. 1 Flow pattern of particle tracer method (pass length 140 mm) Re=500

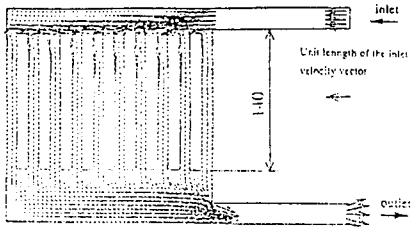

Fig. 16 Velocity vector distribution (pass length 140 mm) Re = 500

CONCLUSION

By searching the uniform distribution of the flow rate to the branch tubes of the heat exchanger, we were able to examine the state of drift in the area of layered flows by using numerical analysis and experimental results.

(1) If the ratio of the total sectional area of the multi-branching tube to the sectional area of the inflow section was relativly high, the flow tended to flow into the nearest branch pass to the outlet port of the outlet chamber.

(2) Even if the length of the branch passes were shortend to increase the volume of the inlet chamber and outlet chamber equally , the decrease in drift was extremely low.

(3) Increment of the volume of the outlet chamber could cease drift only in the area of layered flows.

REFERENCES

(1) T.Ueda and T.Kubo , Bulletin of JSME, Vol. 12, No.52,pp.802-809,1969
(2) S.Ezaki et al. , Transactions of the JSME , Vol. 56 , No. 52 , pp.2247-2256,1990
(3) A.B.Datta and A.K.Majumdar, Int.J.Heat&Fluid Flow Vol.2,No.4,pp.253-262, 1980
(4) R.A.Bajura and E.H.Jones,JR ,Transactions of the ASME Journal of Fluids Engineering, pp. 654-666, December 1976